Characterization of Void Growth in High Temperature Fatigued Copper

Summer School on Neutron Scattering and Reflectometry
From Submicron Structures
NIST Center for Neutron Research
June 26-30, 2006

Abstract

Ultra-small-angle neutron scattering (USANS) will be used to determine the mean void size, the polydispersity in size, and volume fraction of voids in copper. All aspects of the experiment, from the sample preparation and instrument setup through to the data treatment and interpretation will be briefly described and references given for more in-depth study.

I. INTRODUCTION

Characterization of particle size is a common need in the field of materials science. Second phase dispersoids or voids in metal alloys or structural ceramics, and soft matter complexes such as oil-water emulsions have all been studied using small angle scattering. The much higher resolution of the new ultra-small-angle neutron scattering (USANS) instrumentation over conventional SANS extends the maximum particle size from 0.1 to 10 μm (Barker et al., 2005). The extension in the size range provides new opportunities of study not previously available.

It is well known that materials stressed at high temperatures ($0.4\ T_M < T < 0.7\ T_M$ where T_M is the material melting temperature) often fail by the nucleation, growth and coalescence of grain boundary voids (Evans, 1984). The current samples were fatigued at T = 405 C = 0.5 T_M. The stress amplitude had sinusoidal shape with a frequency of 17 cycles per second. The maximum stress amplitude was +/-34 MPa. The grain size is approximately 60 μm. Under the fatigue conditions, the grain boundaries migrate to a preferred diamond morphology where the grain boundaries perferentially lie at 45˚ to the tensile axis. The voids nucleate and grow along the grain boundaries shown schematically in figure 1. Three different samples were fatigued to 2.5e4, 5e4, and 1.0e5 total cycles. The central section was removed from sample. Precision density measurements using Archimede's principle (Ratcliffe, 1965) were used to independently determine the volume fraction of voids ϕ to 10 to 15% accuracy.

Table 1. Three separate copper samples will be measured in this experiment. The number of fatigue cycles, the sample thickness d and the void volume determined from precision density measurements are given below.

# cycles	d	ϕ
25,000	0.605 cm	0.00044 (6)
50,000	0.577 cm	0.00132 (16)
100,000	0.589 cm	0.00241 (40)

Why use SANS?

Generally, static light scattering and small angle X-ray scattering (SAXS) provide the same information about the sample: measurement of macroscopic scattering cross-section $d\Sigma/d\Omega(q)$ as neutron scattering. The contrast in light scattering arises from the difference in the light's refractive index between the particle and water. The wavelength of light limits $q < 0.002$ Å^{-1}. The contrast in X-ray scattering arises from the variation in electron density. For the current copper experiment, neutron or X-ray scattering could be used for size characterization. For x-ray scattering very thin (~ 10 μm) samples would need to be made to accommodate stronger absorption. Static light scattering is not possible due to very strong absorption.

The Objectives of the Experiment are:

- **To determine the size and polydispersity of the voids**. This information will be derived from the shape, i.e. the q-dependence, of the scattering pattern. Since the voids are nearly spherical, it will be necessary in order to characterize the size to measure the intensity over the range $1/D < q < 20/D$, where D is the average diameter of the voids.

- **Determine the volume fraction of the voids**. By integrating the scattering curve, we can determine a quantity called the Porod's invariant. The volume fraction can be determined from Porod's Invariant independent of the void volume. If the mean void volume can be determined separately, the volume fraction can also be resolved from the $q \rightarrow 0$ limit of the scattering curve in absolute units.

- **Determine the surface area from the Porod regime.** The total surface area normalized by the sample volume can be determined from fitting the high Q regime.

II. PLANNING THE EXPERIMENT

Given the stated objectives of the experiment, how do we go about preparing for the experiment to maximize our chances of success? Here we discuss some of the issues that bear on this question.

II.1 Scattering Contrast

In order for there to be small-angle scattering, there must be scattering contrast between, in this case, the void and the surrounding copper matrix. The scattering is proportional to the scattering contrast, $\Delta\rho$, *squared* where

$$\Delta\rho = \rho_p - \rho_w \qquad \leftarrow \text{Scattering Contrast} \qquad (1)$$

and ρ_p and ρ_w are the **scattering length densities** (**sld**) of the voids and the copper matrix, respectively. Recall that **sld** is defined as

$$\rho = \frac{\sum_{i=1}^{n} b_i}{V} \qquad \leftarrow \text{Scattering Length Density} \qquad (2)$$

where V is the volume containing n atoms, and b_i is the (bound coherent) **scattering length** of the i^{th} atom in the volume V. V is usually the molecular or molar volume for a homogenous phase in the system of interest.

The **sld**'s for the two phases in the present case, void and copper, can be calculated from the above formula, using a table of the scattering lengths (such as Sears,1992) for the elements, or can be calculated using the interactive *SLD Calculator* available at the NCNR's Web pages (http://www.ncnr.nist.gov/resources/index.html). The **sld**'s for void and copper are given below in Table 2.

Table 2. The scattering length densities (SLD's) for polystyrene, light water and heavy water.

Material	Chemical Formula	Mass Density (g/cc)	SLD (cm^{-2})
Void	-	0.0	0.0
Copper	Cu	8.94	6.52×10^{10}

II.2 Sample Thickness

The next decision we face is how thick should the sample be? Recall that the scattered intensity, I(q), is proportional to the product of the sample thickness, d, and the sample transmission, T, where T, the ratio of the transmitted beam intensity to the incident beam intensity, is given by

$$T = e^{-\Sigma_t d}, \quad \Sigma_t = \Sigma_c + \Sigma_i + \Sigma_a \qquad (3)$$

where the total cross section per unit sample volume, Σ_t, is the sum of the coherent, incoherent and absorption cross sections per unit volume. The absorption, or neutron capture, cross section, Σ_a, can be computed accurately from the tabulated absorption cross sections of the elements (and isotopes) if the mass density and stochiometry of the phase is known. Σ_a is wavelength dependent, being linearly proportional to λ for nearly all elements. The incoherent cross section, Σ_i, can be *estimated* from the cross section tables for the elements as well, but not as accurately because it depends somewhat on the atomic motions and is, therefore, temperature dependent. The coherent cross section, Σ_c, is not easily estimated since it depends on the details of both the structure and correlated motion of the atoms in the material. The attenuation from copper is dominated by absorption. The USANS instrument uses a neutron wavelength $\lambda = 2.38$ Å, which for copper $\Sigma_a = 0.42$ cm^{-1}. The optimal sample thickness[1], the 1/e thickness, equals $d = 1/\Sigma = 2.3$ cm.

Multiple scattering The scattered intensity is proportional to $d \exp(-\Sigma_t d)$ which has a maximum at $d = 1/\Sigma_t$. But if the small-angle scattering (SAS) intensity is strong enough to create multiple scattering, the scattering curve will become distorted in shape (Schelten & Schmatz, 1980). The sample thickness d should than be chosen to make transmission from only SAS to be $T_{SAS} = \exp(-\Sigma_{SAS} t) > 0.9$ rather than $1/e = 0.37$ to avoid multiple scattering. The cross-section due to SAS can be calculated for monodisperse spheres as

$$\Sigma_{SAS} = \tfrac{3}{4} \lambda^2 \phi \Delta\rho^2 D \qquad (4)$$

where ϕ is the volume fraction and D is the sphere diameter. The voids in these samples have a broad size distribution around 1 μm diameter, and volume fraction of 0.1 %. Using equation 4, $\Sigma_{SAS} \approx 0.2$ cm^{-1}. To keep the transmission from SAS $T_{SAS} > 0.9$, $d < 0.1/\Sigma_{SAS} = 0.5$ cm.

II.3 Required Q-Range

For this experiment we know we will need to measure the intensity over a wide q-range since the information we are looking for is distributed in the low and high q regime. To get a better idea of the required q-range, we can use the *SANS Data Simulator* (http://www.ncnr.nist.gov/resources/simulator.html) to calculate the Q-dependence of the scattering for the case of non-interacting polydisperse spherical particles. From among the 20 different particle models currently included in the *SANS Data Simulator*, we choose the *Polyhardsphere* model. The documentation for this model can be found on the Web site at http://www.ncnr.nist.gov/resources/sansmodels/polyhardsphere.html. A plot from the *SANS Data Simulator* for 1 vol % spheres with polydispersity ($p=\sigma/D$) in sphere diameter of p = 0, 1.3% and 5% are shown in Figure 2. Note how with increasing polydispersity, the minima in scattering function are attenuated. Determination of the polydispersity from SAS data requires accurate measurement of the oscillating section of scattering curve.

III. COLLECTING THE DATA

Figure 3 shows the schematic layout of the instrument. The sample is placed in a five-position sample changer. A channel cut silicon crystal (monochromator) provides a neutron beam onto the sample with excellent angular collimation (2 arcsec) in the horizontal direction, but with poor resolution in the vertical direction. To select a scattering angle, a second channel-cut silicon crystal (analyzer) is rotated. The main detector than collects scattering with high resolution in horizontal direction. Figure 4 represents the q-resolution obtained using the USANS double crystal diffractometer.

III.1 How to Configure the USANS Instrument

The USANS instrument collects data at one value of q at a time. Thus, we need to choose all the q-values to count during the experiment. Since we need to cover an extended Q-range, $5x10^{-5}$ $Å^{-1} < q < 5x10^{-3}$, we break the data collection into six separate equally spaced scans, with each subsequent scan having roughly doubled q-spacing. The first scan spans the main beam. The peak intensity is used to determine the q=0 orientation, scales the intensity into absolute units, and determines the sample transmission.

III.2 Sample Transmission

The sample transmission is determined in two ways. A separate transmission detector (see figure 3), located behind the analyzer, collects all neutrons transmitted through the analyzer. When the analyzer is rotated a sufficient angle off of main beam orientation, the transmission detector collects both the direct beam intensity, and the small angle scattered intensity. The ratio of counts collected with the transmission detector, with and without the sample, is the sample transmission (T_{wide}) due to attenuation from incoherent scattering and absorption. In addition, rotating the analyzer through the orientation of the main beam measures only the beam intensity in the main detector. Thus the peak intensity measured with the sample measures the transmission (T_{rock}) of the sample due to attenuation from incoherent scattering, absorption and *small angle (coherent) scattering.*

The ratio of these separate transmission measurements can be used to estimate the amount of multiple scattering by determining the scattering power ($\tau = \Sigma_{SAS}t$) by

$$T_{SAS} = \frac{T_{Rock}}{T_{Wide}} = e^{-\tau} \qquad (5)$$

III.3 What Measurements to Make

To correct for instrument "background", measurement of the scattering without the sample is needed. Counts recorded by the detector with the sample in place can come from three sources: 1) neutrons scattered by the sample itself (the scattering we are interested in); 2) neutrons scattering from something other than the sample, *but which pass through the sample*; and, 3) everything else, including neutrons that reach the detector *without passing through the sample* (stray neutrons or so-called room background) and electronic noise in the detector itself. To separate these three contributions, we need three measurements:

i) Scattering measured with the sample in place (which contains contribution from all 3 sources listed above), denoted $\mathbf{I_{sam}}$;

ii) Scattering measured with the empty sample holder in place (which contains contributions from the 2nd and 3rd sources listed above), denoted $\mathbf{I_{emp}}$; and,

iii) Counts measured with a complete absorber at the sample position (which contains only the contribution from the 3rd source listed above) denoted $\mathbf{I_{bgd}}$.

The I_{bgd} on the USANS instrument is due predominantly to fast neutrons. This background is independent of instrument configuration and is 0.018 s^{-1} = 0.62 / 10^6 monitor counts. For this reason, separate beam blocked runs are generally not made for the USANS instrument.

III.4 How Long to Count

A SANS experiment is an example of the type of counting experiment where the uncertainty, or more precisely the standard deviation, σ, in the number of counts recorded in time, *I(t)*, is $\sigma = \sqrt{I(t)}$. Increasing the counting time by a factor of four will reduce the relative error, σ/I, by a factor of two. If there are 1000 total counts per data point, the standard deviation is $\sqrt{1000} \sim 30$, producing an relative uncertainty of about 3 %, which is good enough for most purposes.

A related question is how long should the empty cell measurements be counted relative to the sample measurement. The same $\sigma = \sqrt{I(t)}$ relationship leads to the following approximate result for the optimal relative counting times

$$\frac{t_{background}}{t_{sample}} = \sqrt{\frac{Count\ Rate_{background}}{Count\ Rate_{sample}}} \; . \qquad (6)$$

Hence if the scattering from the sample is weak, the background should be counted for as long (but no longer!) as the sample scattering. However, if the sample scattering count rate is, say, 4 times greater than the background rate, the background should be counting only half as long as the sample scattering.

Since the scattering usually becomes much weaker at larger q, the time spent per data point is greatly increased with higher q scans.

IV. DATA REDUCTION

Data reduction consists of correcting the measured scattering from the sample for the sources of background discussed in Section III.3, and rescaling the observed corrected data on an absolute scale of scattering cross section per unit volume. The scaling of the slit smeared background-corrected neutron count rate, $I_{cor}(q)_S$, to the slit smeared absolute cross section, $d\Sigma_S(q)/d\Omega$, is done through the expression

$$I_{cor}(q)_S = \varepsilon\, I_{Beam}\, \Delta\Omega_A\, d\, T\, (d\Sigma_\Sigma(q)/d\Omega)\,, \qquad (7)$$

Where:

ε = detector efficiency.
I_{beam} = The intensity of the beam incident upon sample (neutrons/sec)
d = the sample thickness
T = the transmission of the sample (and its container, if there is one)
$\Delta\Omega$ = the solid angle accepted by analyzer
$d\Sigma_S(q)/d\Omega$ = slit smeared scattering cross-section.

The beam intensity, $\varepsilon\, I_{Beam}$, is measured by rotating analyzer through the direct beam at q = 0 with the empty cell in the beam. The transmission T is measured by taking the ratio of count rate obtained with and without the sample in the beam with transmission detector. The solid angle of scattering collected by the analyzer is

$$\Delta\Omega_A = \left(\frac{\lambda}{2\pi}\right)^2 (2\Delta q_V)\Delta q_H, \qquad (8)$$

where $2\Delta Q_V$ is the total vertical divergence of the beam convoluted with angular divergence accepted by the detector, and Δq_H is the horizontal divergence accepted by diffraction of monochromator and analyzer crystals. The instrument accepts scattered neutrons with +/- $\mathbf{\Delta q_V = 0.117\ \AA^{-1}}$ divergence in terms of momentum transfer q. The horizontal resolution Δq_H is measured from the full width at half maximum (fwhm) of the main beam profile obtained by rotating analyzer through direct beam. The fwhm is 2.00 arcsec, producing $\Delta q_H = 2.55\text{x}10^{-5}$ $\AA^{-1}$. The solid angle accepted by the analyzer is $\mathbf{\Delta\Omega_A = 8.6\text{x}10^{-7}}$ **Ster**.

<u>Smearing</u>

The analyzer has good resolution in only one direction, as shown in figure 4. The measured smeared cross-section $d\Sigma/d\Omega_S(q)$ is related to desired true cross-section $d\Sigma/d\Omega(q)$ by the relation (Roe, 2000)

$$\frac{d\Sigma_S}{d\Omega}(q) = \frac{1}{\Delta q_V}\int_0^{\Delta q_V} \frac{d\Sigma}{d\Omega}\left(\sqrt{q^2+u^2}\right)du \tag{9}$$

Figure 5 shows the slit-smeared scattering from spherical particles having $\phi = 0.01$ with p = 0.0, 0.013 and 0.05. Compare this to the 'true' scattering shown in figure 2. Infinite slit smearing tends to dampen the oscillations. Desmearing the data directly can be done by an iterative convergence method (Lake,1967). The desmeared result is very unstable, being sensitive to noise in the data. In our analysis we will fit the smeared data *directly*.

V. DATA ANALYSIS

V.1 Modeling the Scattering

Since the volume fraction of the voids in our samples is about 0.001, it is reasonable to analyze the scattering in terms of non-interacting particles. For higher volume fractions, the correlation in particle positions must be considered. Exclusion of possible positions due to impenetrability of the hard spheres can be modeled by Percus & Yevick, 1958. Charge stabilization can cause larger effects at even relatively dilute concentrations (Chen & Lin, 1987). In the so-called dilute limit, the particles scatter independently, and the total scattering is the sum of the scattering from each particle. The measured intensity (corrected for background and put on an absolute scale) for monodisperse spherical particles can be expressed as

$$\frac{d\Sigma(q)}{d\Omega} = \Delta\rho^2\left\langle V_p^2\right\rangle N_p P(q), \tag{10}$$

where $\Delta\rho$ is the difference in sld's between the polystyrene particles and D_2O; $\langle V_p^2\rangle$ is the mean particle volume squared, and N_p is the number of particles per unit volume. $P(q)$ is the scattering form factor, which for spherical particles is

$$P(q,R) = \left|\frac{1}{V_p}\int_{V_p} e^{i\vec{q}\cdot\vec{r}}d\vec{r}\right|^2 = \left[\frac{3(\sin qR - qR\cos qR)}{(qR)^3}\right]^2 = \tag{11}$$

where R is the sphere radius. The scattering from a size distribution f(R) of particles is

$$\frac{d\Sigma(q)}{d\Omega} = \left(\frac{4\pi}{3}\right)^2 \Delta\rho^2\ N_p\int f(R)R^6P(q,R)dR \tag{12}$$

Since the current sample is relatively monodisperse, we will approximate the shape of the distribution with a gaussian:

$$f(R) = \frac{1}{\sigma\sqrt{2\pi}} \exp\left[-\frac{1}{2\sigma^2} \left(R - R_{avg} \right)^2 \right] \tag{13}$$

where R_{avg} is the mean particle radius. We define $p = \sigma / R_{avg}$.

V.2 Particle Volume Fraction Determined from Invariant

For all two phase systems having uniform scattering length densities in each phase, the volume fraction ϕ can be determined from the integration of the scattering

$$\phi(1-\phi) = \frac{Q_I}{2\pi^2 \Delta\rho^2} \tag{14}$$

where the invariant is determined by

$$Q_I \equiv \int_0^\infty q^2 \frac{d\Sigma}{d\Omega}(q) dq \cong \frac{1}{\Delta q_v} \int_0^\infty q \frac{d\Sigma_s}{d\Omega}(q) dq \tag{15}$$

Figure 6 shows an *invariant* plot of the slit-smeared scattering: $qI_S(q)$ vs q. By integrating the area under the curve, we will be able to determine the Porod invariant Q_I and subsequently the volume fraction ϕ. This technique of determining the volume fraction from scattering data works regardless of particle shape.

V.3 Particle Volume Fraction Determined from Forward Scattering

For dilute systems, and if the particle has a uniform scattering length density, the forward scattering is simply:

$$\frac{d\Sigma}{d\Omega}(0) = N_P \left\langle V_P^2 \right\rangle \Delta\rho^2 = \frac{4}{3} \pi\phi\Delta\rho^2 \frac{\left\langle R^6 \right\rangle}{\left\langle R^3 \right\rangle} = \frac{4}{3} \pi\phi\Delta\rho^2 R_{avg}^3 \frac{\left(1 + 15p^2 + 45p^4 + 15p^6 \right)}{\left(1 + 3p^2 \right)} \tag{16}$$

where ϕ is the volume fraction of particles, V_P is the average particle volume, and $\Delta\rho^2$ is the scattering length density contrast squared. By slit-smearing Guinier approximation, we can estimate the forward scattering $d\Sigma/d\Omega(0)$ directly from slit smeared intensity by

$$\frac{d\Sigma}{d\Omega}(0) \approx \frac{2 R_G \Delta q_V}{\sqrt{3\pi}} \frac{d\Sigma_S}{d\Omega}(0) \tag{17}$$

Since we know R_{avg}, p, and $\Delta\rho$, and $d\Sigma/d\Omega(0)$ from equation 17, we can determine the volume fraction ϕ. We will determine $d\Sigma_S/d\Omega(0)$ by performing a Guinier fit, described later in section V.5.

V.4 Determination of the Interfacial Surface Area:

Total interfacial surface area is determined from small angle scattering data using Porod's asymptotic approximation:

$$\lim_{q\to\infty}\frac{d\Sigma}{d\Omega}(q)\equiv C_P/q^4=2\pi\,\Delta\rho^2\,S/q^4 \tag{18}$$

where *S* is the interfacial surface area per unit sample volume. The slit smeared intensity in the Porod region is modeled as

$$\lim_{q\to\infty}\frac{d\Sigma_S}{d\Omega}(q)\equiv C_{P,S}/q^3=\frac{\pi C_P}{4\Delta q_V q^3} \tag{19}$$

For a Gaussian distribution of sizes

$$S=4\pi\left\langle R^2\right\rangle N_P=3\phi\frac{\left\langle R^2\right\rangle}{\left\langle R^3\right\rangle}=\frac{3\phi}{R_{avg}}\frac{\left(1+p^2\right)}{\left(1+3p^2\right)} \tag{20}$$

Figure 7 shows the slit-smeared Porod plot: $q^3I(q)$ vs q. By determining an average value between oscillations, we can determine $C_{P,s}$, C_P and subsequently S. Using equation 20, we can than determine the volume fraction ϕ.

V.5 Determination of Particle size from Guinier Law:

In the Guinier limit $q\to 0$, the above expressions 8-10 simplify to

$$\frac{d\Sigma}{d\Omega}(q)=\frac{d\Sigma}{d\Omega}(0)\exp(-q^2R_g{}^2/3)$$

$$R_G=\sqrt{\frac{3\left\langle R^8\right\rangle}{5\left\langle R^6\right\rangle}}=R_{avg}\sqrt{3/5}\frac{\left(1+28p^2+210p^4+420p^6+105p^8\right)}{\left(1+15p^2+45p^4+15p^6\right)} \tag{21}$$

The above equation is an example of Guinier's Law which is valid only for $q\,R_g \le 1$, where R_g is the radius of gyration of the particle. **For a homogenous sphere, $R_g^2 = 3R^2/5$.** This expression is easy to use and allows us to quickly extract the radius of gyration of particles in the low q region by plotting *ln(I)* versus q^2. Figure 8 shows the scattering using a Guinier plot. Note that slit smearing does not change the slope of curve, but shifts the curve vertically according to equation 17.

V.6 Summary of Analysis Tasks

We shall perform the following fits to the slit smeared scattering $d\Sigma_S/d\Omega(q)$ data:

1) Use a Gaussian shaped size distribution of spheres to determine mean sphere size R_{avg} , the polydispersity P and the volume fraction ϕ. Equations 10-13 are used.

2) Integrate the scattering according to equation 15 to determine Porod's invariant Q_I. The invariant will be used to determine the volume fraction ϕ using equations 14 and 15.

3) Perform a Guinier fit to the data as shown in figure 8. The slope will be converted to a Guinier radius R_G which can than be used to calculate the mean particle radius R_{avg}. The forward cross-section, corrected for smearing by equation 17, will be used to calculate the volume fraction ϕ.

4) Make a Porod plot and determine asymptotic Porod's constant $C_{P,s}$. From equations 18 and 19 determine interfacial surface area S. From know average particle size, determine volume fraction using equation 20.

From the above fits, we will have one determination of polydispersity P, two determinations of mean particle size R_{avg} , and four separate determinations of volume fraction.

VI. REFERENCES AND OTHER RESOURCES

Barker, J.G., Glinka,C.J., Moyer, J.J., Kim, M.H., Drews, A.R., & Agamalian, M. *J. Appl. Cryst.* **38**, 1004-1011 (2005).

Chen, S.-H. & Lin, T.-L. *Methods of Experimental Physics*, **23B**, 489-543 (1987).

Evans, H.E. *Mechanisms of Creep Fracture,* Elsevier Applide Science Pub. (1984).

Lake, J. *Acta Cryst.*, **23**, p191-194 (1967).

Percus, J.K. & Yevick, G.J. *Phys. Rev.* **110**, 1-13 (1958).

Ratcliffe. R.T. *Brit. J. Appl. Phys.* **16** 1193-1196 (1965).

Roe, R.J. *Methods of X-Ray and Neutron Scattering in Polymer Science*, Oxford University Press, (2000).

Schelten, J. & W. Schmatz, *J. Appl. Cryst.*. **13**, p385-390 (1980).

Sears, V.F. *Neutron News*, **3**, No. 3, p 26 (1992).

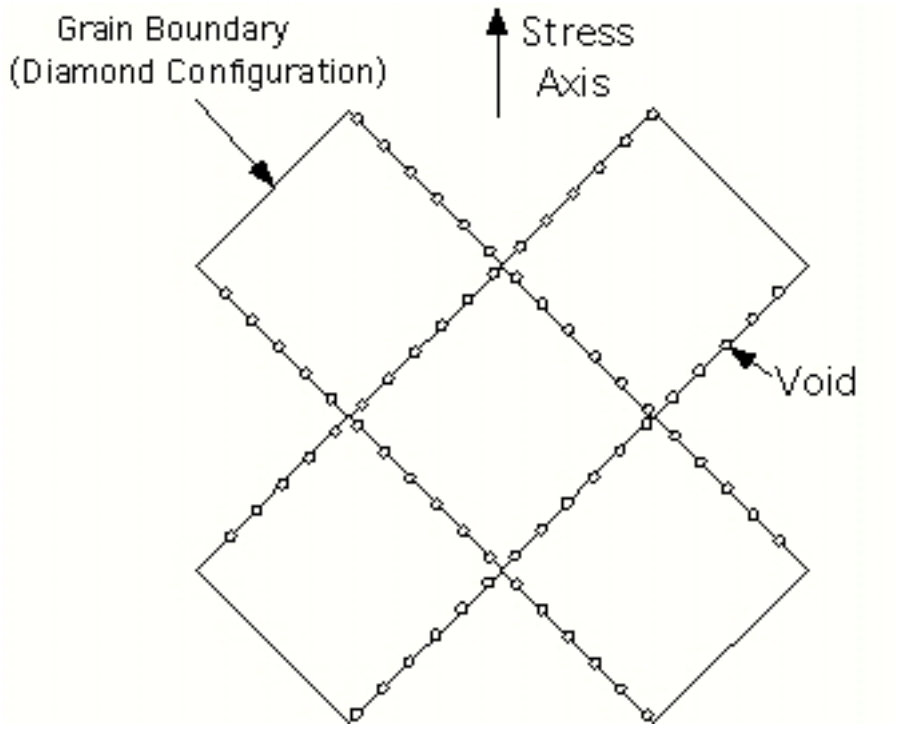

Figure 1. A simplified drawing detailing the preferred the alignment of grain boundaries in a diamond configuration 45˚ to the stress axis. On a lrage fraction of the grain boundaries, voids nucleate and grow. At a late stage, the cavities link up to form grain size cracks.

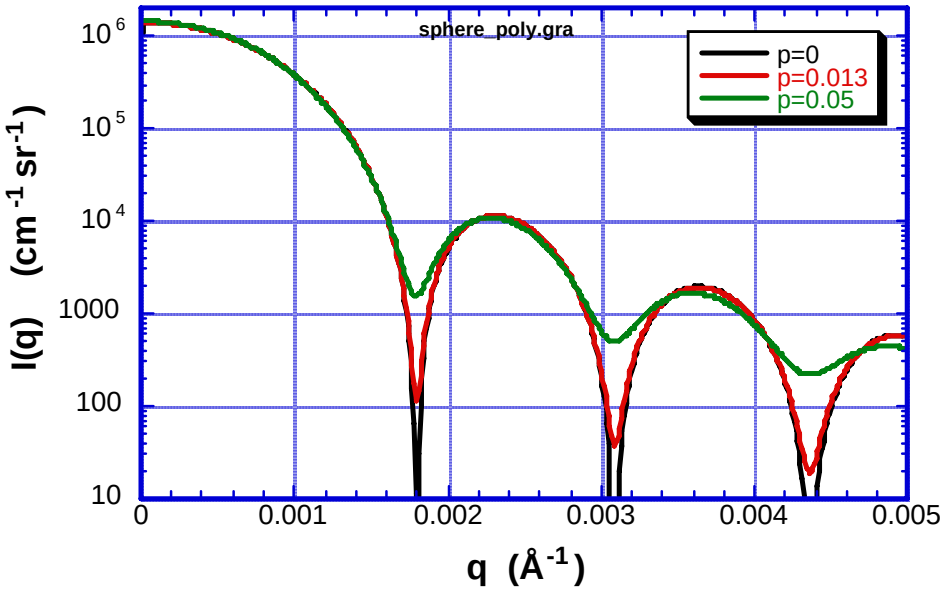

Figure 2. The simulated SANS from polydisperse spheres with diameter D = 5000 Å. Three different polydispersities are included (P = 0 (monodisperse), 1.3 % and 5 %).

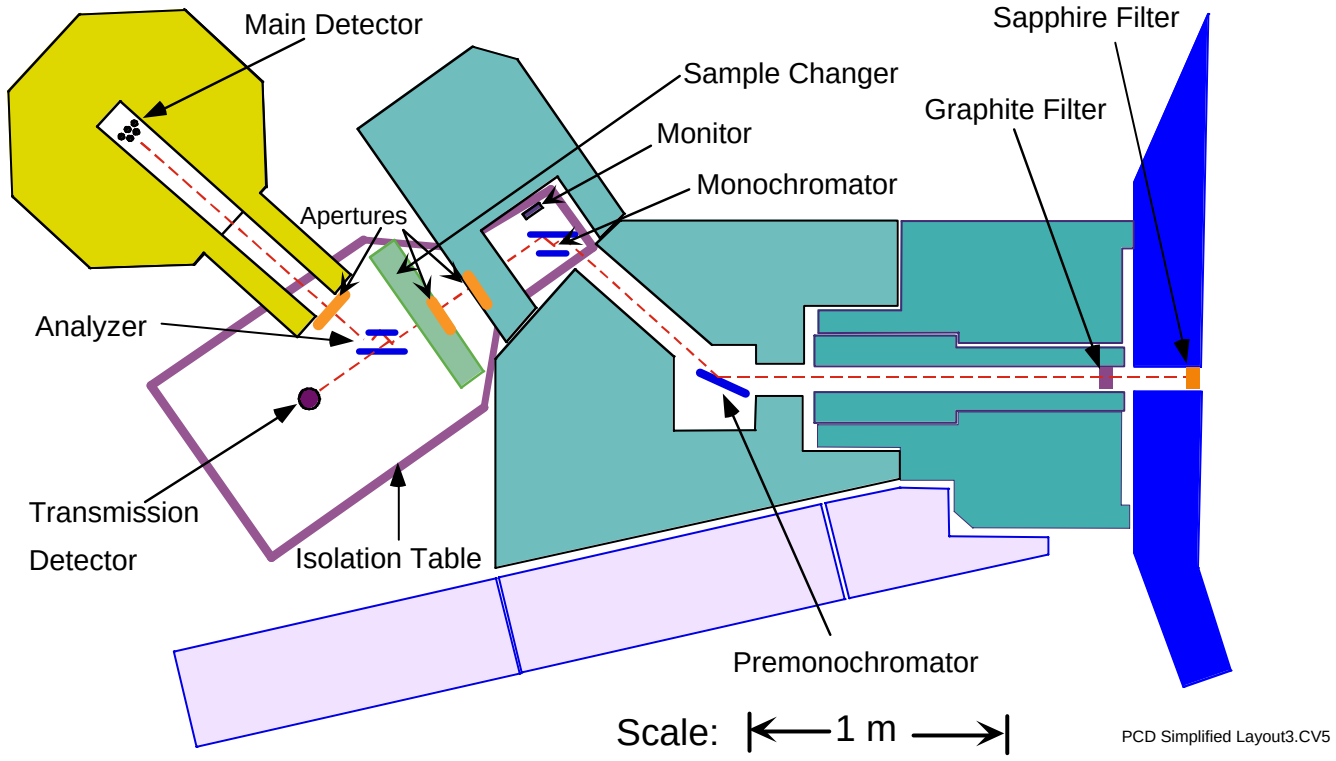

Figure 3. Figure of the schematic layout of the USANS instrument. The dashed line indicates the beam path. The measured scattering angle, or momentum transfer q, is determined by rotation of analyzer crystal.

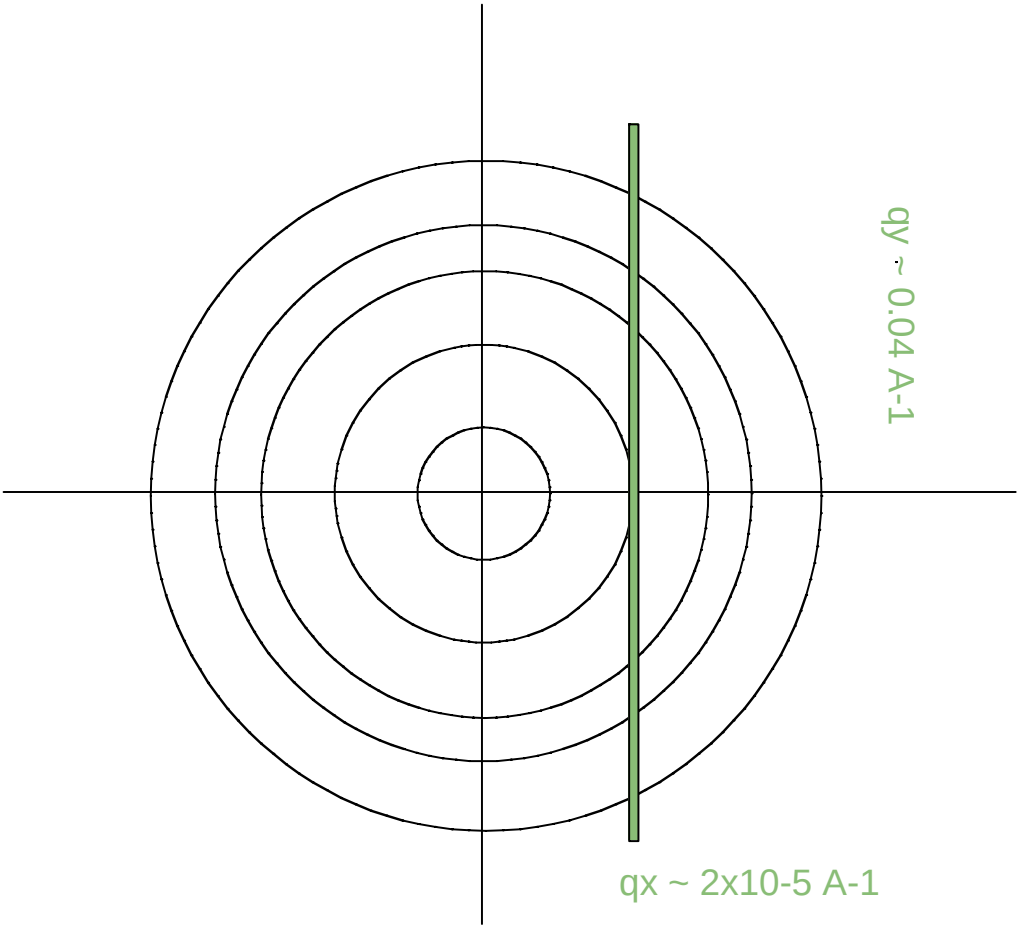

Figure 4. View of scattering with axis q_x and q_y collected by analyzer on USANS instrument. Circles represent iso-intensity contours from isotropic small angle scattering. The narrow slit represents the scattering region collected by analyzer.

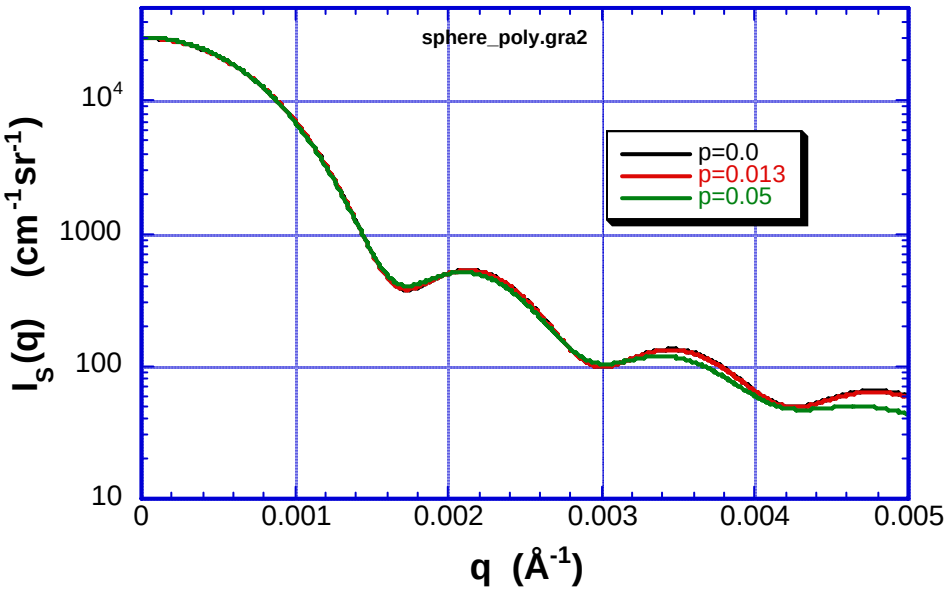

Figure 5. Slit smeared scattering cross-section for spherical particles, R_{avg} =2495 Å, for polydispersity p =0, 0.013 or 0.05. The slit length for smearing was Δq_V = 0.037 Å^{-1}.

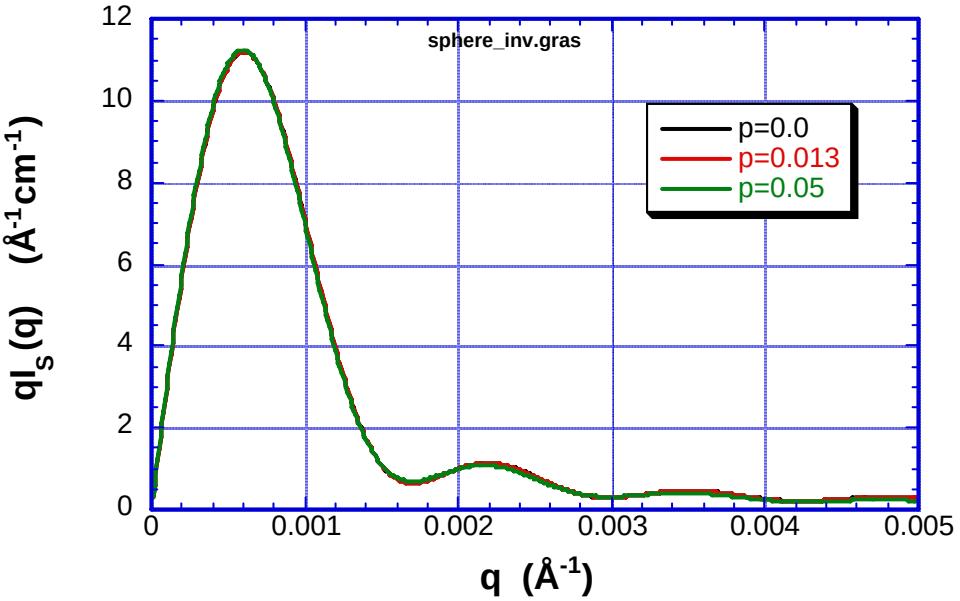

Figure 6. Invariant type plot of slit smeared data: $qI_S(q)$ vs q. The area under curve is proportional to the Porod invariant Q_I which can be used to calculate volume fraction.

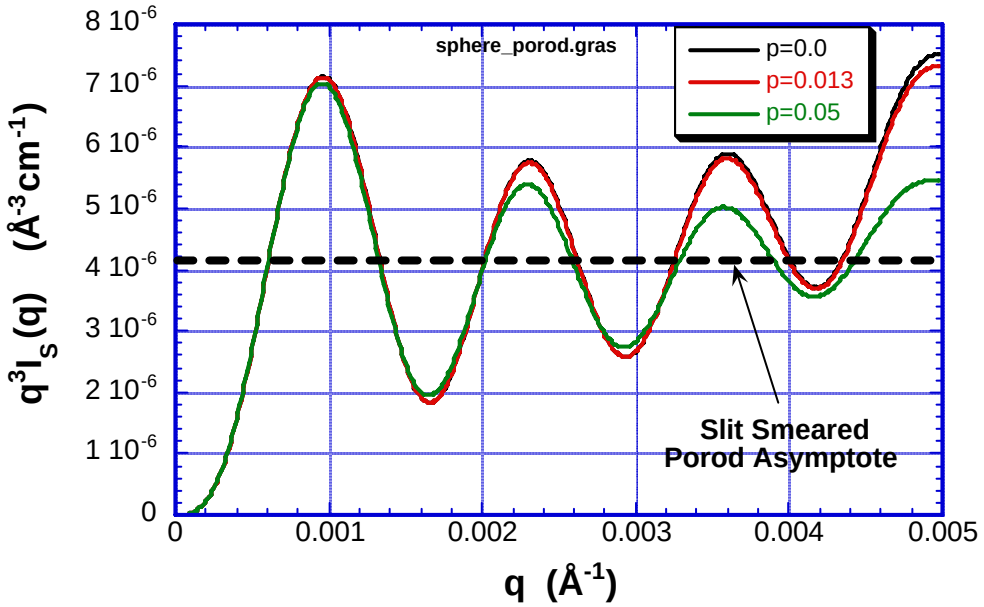

Figure 7. Porod type plot of slit smeared data: $q^3 I_S(q)$ vs q. The dashed curve is the average value of asymptotic data: $C_{P,S}$.

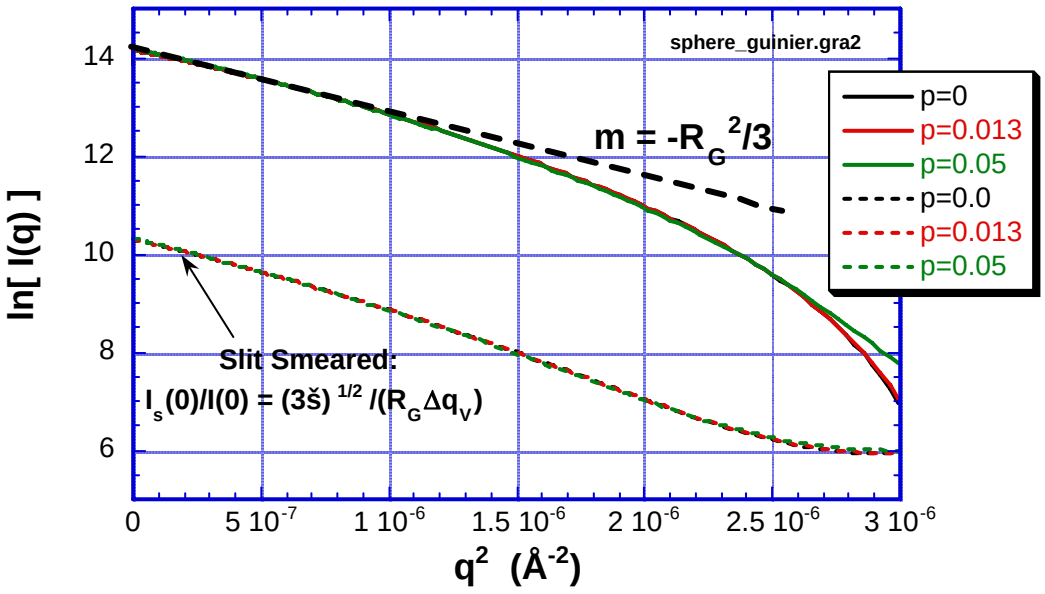

Figure 8. Plot showing Guinier fit to model data [ln(I) vs. q^2]. Fit made in small q limit: $0 < q < 1.2/R_G$. Dashed curves show effect of slit smearing.